A 4-D dataset for validation of crystal growth in a complex three-phase material, ice cream

2015 IOP Conf. Ser.: Mater. Sci. Eng. 84 012076

(http://iopscience.iop.org/1757-899X/84/1/012076)

A 4-D dataset for validation of crystal growth in a complex three-phase material, ice cream

P. Rockett[1], S. Karagadde[1,2], E. Guo[1], J. Bent[3], J. Hazekamp[3], M. Kingsley[1], J. Vila-Comamala[4], and P.D. Lee[1,*]

[1] School of Materials, The University of Manchester, Manchester, M13 9PL, U.K
[2] Department of Mechanical Engineering, Indian Institute of Technology Bombay, Mumbai 400076, India
[3] Unilever R&D, Colworth, U. K
[4] Diamond Light Source Ltd., Harwell Science and Innovation Campus, Didcot, OX11 0DE, U.K

* Corresponding Author: Peter.Lee@manchester.ac.uk

Abstract. Four dimensional (4D, or 3D plus time) X-ray tomographic imaging of phase changes in materials is quickly becoming an accepted tool for quantifying the development of microstructures to both inform and validate models. However, most of the systems studied have been relatively simple binary compositions with only two phases. In this study we present a quantitative dataset of the phase evolution in a complex three-phase material, ice cream. The microstructure of ice cream is an important parameter in terms of sensorial perception, and therefore quantification and modelling of the evolution of the microstructure with time and temperature is key to understanding its fabrication and storage. The microstructure consists of three phases, air cells, ice crystals, and unfrozen matrix. We perform *in situ* synchrotron X-ray imaging of ice cream samples using in-line phase contrast tomography, housed within a purpose built cold-stage (-40 to +20°C) with finely controlled variation in specimen temperature. The size and distribution of ice crystals and air cells during programmed temperature cycling are determined using 3D quantification. The microstructural evolution of three-phase materials has many other important applications ranging from biological to structural and functional material, hence this dataset can act as a validation case for numerical investigations on faceted and non-faceted crystal growth in a range of materials.

1. Introduction

Ice cream is a complex multi-phase material that roughly consists of 30% ice, 50% air, 5% fat and 15% sugar solution matrix, by volume, and thus contains the three states of matter – solid, liquid and gas. This investigation seeks to gain an informed understanding of the manner in which phase content alters with progressive temperature variation [1,2]. However, as far as structure is concerned the quality of the product is generally assumed to depend on the size of the constituent air cells and ice crystals, in both cases the smaller the better. Under abusing temperature variations that commonly occur during storage and distribution, the size of these two components are known to increase. In particular, ice crystallization has an important bearing on ice cream shelf life [3]. An understanding of the mechanisms behind ice formation would greatly aid manufacturers in predicting the effects of processing and in the development of formulations. The observation of ice crystallization is beset with technical difficulties given the opaque and delicate labile nature of ice cream. For optical, or electron

microscopic, relatively extensive alteration to the original composition is involved and in consequence diminishes the value of the resultant measurement. Fortunately, the application of X-ray microtomographic analysis can provide a non-invasive means of observation of three-dimensional structure and in most cases is able to sustain a natural environment. The results discussed in this report were obtained at the Diamond Light Source, using pink beam X-ray tomographic imaging on the Diamond Manchester Branchline (DMB). With filtered undulator harmonics pink beam combines the high intensity required for real time imaging dynamics coupled with a sufficient narrow energy window for high-resolution in-line phase contrast [4].

The motivation for this work is to encourage the application of analytical techniques that would be new to soft solid colloidal materials research but that are commonly employed in other disciplines such as metallic [5–9] and non-metallic [10–12] materials research. Some recent studies have also been performed using laboratory X-ray imaging [13,14]. In this respect the intention is to provide a series of datasets as a gold standard for analysis and model validation. The datasets comprise continuously recorded tomographic reconstructions of ice cream that have undergone phase change structural reorganization during a sequence of heating and cooling cycles. In particular this data will contain information of the dynamics of recrystallization of ice crystals and the coarsening of air cells that result from thermal abuse.

In order to subject a specimen of ice cream to the desired thermal conditions and at the same time provide the appropriate containment and rotational motion required for tomographic projection, a specialized cold-stage was developed for installation on the DMB. The method of temperature reduction was based upon heat extraction by thermoelectric cooling devices and temperature variation on controlled heat input from miniature resistance heaters. The translational and rotational motion instrumentation available on the DMB was incorporated in the cold-stage design to accurately manipulate the ice cream specimen. To match the intrinsic field of view of the beamline instrumentation the ice cream specimens were contained within polyetherimide (PEI) tubes of 3 mm inner diameter with 0.2 mm wall thickness and 10.5 mm length. With this arrangement the specimens could be subjected to temperature variation in the range from ambient values to -40°C with an accuracy of 0.1°C.

2. Methods:

2.1. Ice Cream preparation details

500 ml blocks of 5% fat ice cream were prepared using a scraped surface heat exchanger. The sample tubes were inserted into the ice cream before blast freezing at -35°C and subsequent storage at -25°C. The ice cream filled PEI tubes were cut from the block of ice cream on a bed of dry ice shortly before X-ray analysis.

2.2. Specimen Cold-stage

The specimen cold-stage provides temperature variation from ambient conditions to -40°C with a controlled accuracy approaching 0.1°C. The sample is mounted within a thermally radiating enclosure located within a copper cold block (see Fig. 1). The enclosure is sealed with thermally reflecting aluminium foil X-ray transmission windows at the entrance and exit of the X-ray path. The geometry of the coupling between the cold-block and the rotation spindle is chosen to incorporate existing beam-line and lab systems motion control stages. This approach preserves the proven features of the specimen-mounting arrangements and maintains the accuracy of the specimen transverse location and specimen rotation. In this respect the specimen rotation spindle is mounted on existing rotation stages and vertically loaded into the cold-block assembly. A contact angle of 5° between the spindle cone and a conical recess in the cold block provides a suitably conductive thermal path with accurate location. This geometry also allows spindle rotation with acceptable levels of motion friction.

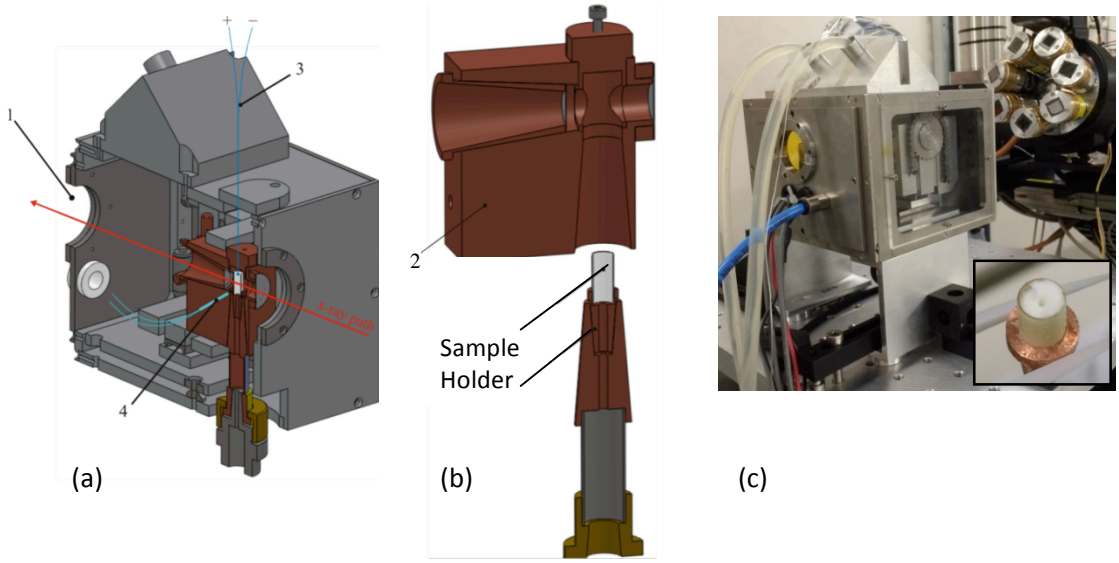

Fig 1: (a) Sectional view of the cold stage assembly (1-X-ray window; 2-Cold block; 3-Outer aluminium casing; 4-Platinum resistance thermometers) (b) Sample mounting and positioning (c) Picture of the cold stage installed in the Diamond Manchester Branchline, with the inset showing a typical sample.

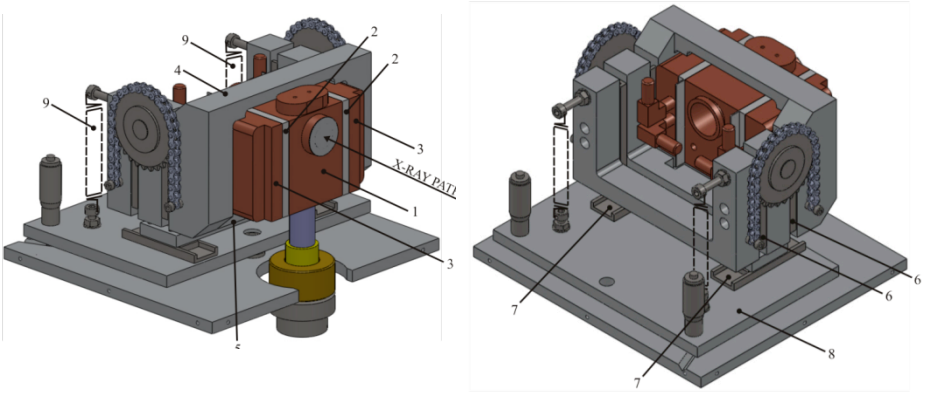

Fig 2: Cold-stage assembly mounted on three-axis slide system. 1-cold block, 2-thermoelectric coolers, 3-water cooled heat exchangers, 4-cooler compression frame, 5-lateral slides, 6-vertical slides, 7-longitudinal slides, 8-pitch and roll plate, 9-counter load springs

The cold block is sandwiched between two 70 W, 40 × 40 mm, planar thermoelectric cooling elements (Marlow Industries, Texas, USA) and held into position under soft compression by two water-cooled heat exchangers that remove heat from the cooling elements (Fig 2). To ensure that the alignment of the rotation stage determines the accurate location of the specimen spindle, the cold-block assembly is freely floating on a three-axis arrangement of miniature linear motion slides. The cold block assembly is mounted on a pitch and roll plate for micrometer alignment of the rotation spindle axis and the cold block recess axis. Two springs are attached between a vertical sliding frame and the pitch/ roll plate to provide adjustable load relief to the rotation spindle via circulating miniature chains.

To provide compatible combinations of image resolution and area the sample containment tubes vary in diameter from 3 – 5 mm. The tubes are fabricated from polyetherimide (PEI, Goodfellow,

Cambridge, UK) with 0.2 mm wall thickness and 10.5 mm length. These fit into a recess in a copper support capsule that conically locates in the top of the rotation spindle. The geometry of the cold-stage system has been structured to allow sample loading either from the top or from the bottom of the system, Fig 1(b).

The cold-stage assembly is housed within an environment chamber. A controlled gas bleed (~0.15 bar) prevents water droplet condensation and maintains the pressure at slightly above ambient so that seals are not required at the rotation spindle entry aperture and any other smaller access ports. Very soft flexible tubing is used for the heat exchanger water coolant and feed into the chamber in an unconstrained manner in order not to restrict the free movement of the cold block assembly. Two P100-type platinum resistance thermometers are inserted in the cold-block, as close as possible to the specimen support capsule, and a K-type thermocouple is inserted through the top of the cold-block assembly to monitor the specimen temperature.

Four 16 W cartridge heaters (Watlow, UK) are inserted at the rear of the cold-block to provide temperature control. The principle of operation is to set the thermoelectric cooler heat out-flux to a fixed value and to control the temperature of the cold-stage to the programmed set point with heat in-flux determined under computer control. The temperature controller (ITC503, Oxford Instruments, UK) is provided with 64 W of heater power and three input channels for sensor monitoring. Two channels were calibrated for P100-type platinum resistance thermometer inputs and one channel was calibrated for K-type thermocouple input. The system could be operated in either a local or remote control. The remote temperature control was implemented with a National Instruments 4-Port Ethernet Interface for RS232 (ENET-232/4). In this manner variable temperature sweep profiles could be programmed.

2.3. Synchrotron X-ray computed microtomography (SXMT)

Synchrotron X-ray tomography of the ice cream microstructure was performed on the Diamond Manchester Branchline at the Diamond Light Source, operating with a pink beam. The pink beam provides high flux undulator radiation with relatively small energy dispersion so that both high temporal and spatial resolution are available to perform 4D in-line phase contrast imaging [4]. A 2560 × 2160 pixel PCO Edge 5.5 CMOS camera optically coupled to a single crystal $CdWO_4$ scintillator resulted in a resolution of 1.6 μm / pixel. For the tomography, a total of 3600 projections were obtained over a 180° rotation with an exposure time of 0.1 s. For optimum image resolution the distance between the sample and the scintillator was ~13 mm. Back-projection reconstruction of the recorded tomographic projection datasets was performed using a combined Fourier-wavelet algorithm to suppress ring artefacts [15]. The reconstructed volume was 2560 × 2568 × 2160 voxels. The 2D images were processed and analysed with ImageJ. 3D visualization was made using Avizo®, FEI-VSG, France.

2.4. Experimental procedure

For long-term storage the ice cream samples, contained within 3 mm diameter PEI tubes, were stored in a -80°C freezer. Typically, a sample was mounted in the cold stage and stabilized at -20°C for ten minutes, after which a tomographic scan was recorded to determine the initial state. Following this the temperature was increased, at a ramp rate of 0.3°C/min, to -8°C and held there for 10 minutes. The sample was then cooled, at the same ramp rate, back to the base temperature of -20°C, after which a tomographic scan was recorded. The thermal cycle was repeated for the same sample but with the highest temperature now set at -7°C. This procedure of repetitive thermal cycling, as shown in Fig 3, contains features that are common to the temperature abuse of ice cream associated with incorrect storage handling.

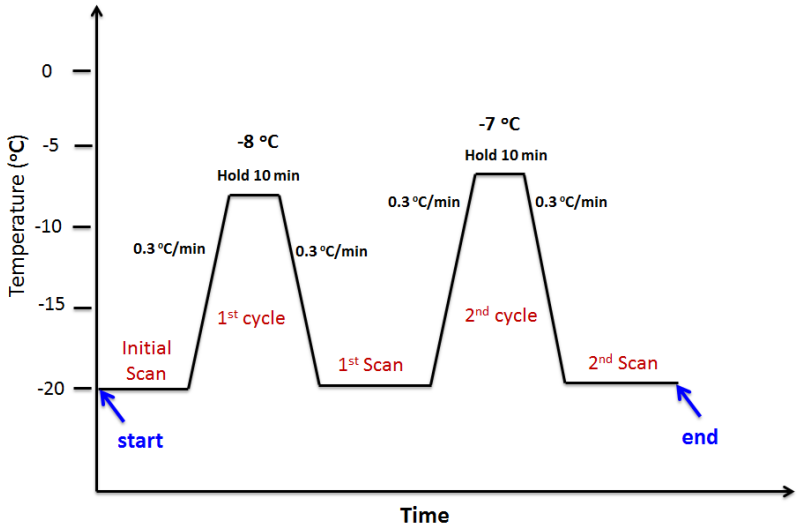

Fig 3: Schematic of the thermal cycling of the ice cream sample and the actions taken at each stage

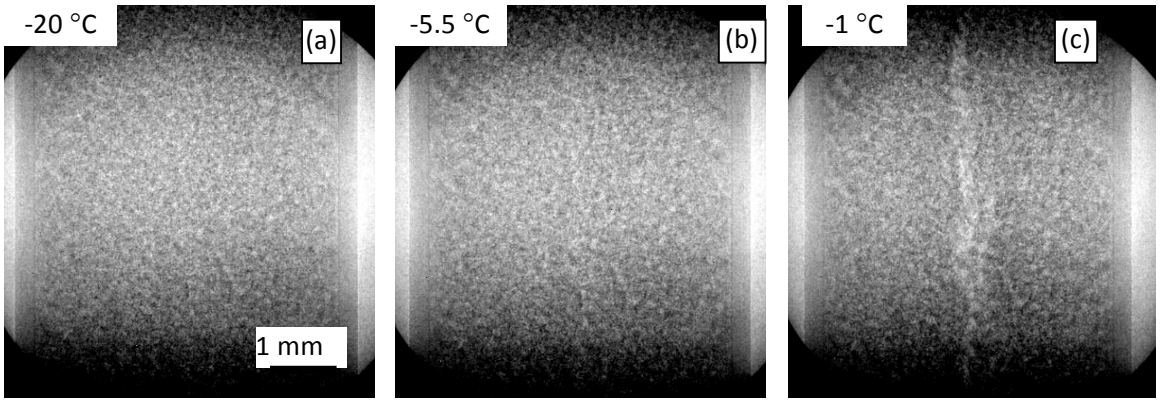

Fig 4: Radiographs of a 3 mm sample during a heating cycle from -20 to 0 °C at 0.1 °C/min: the images were taken at temperatures (a) -20, (b) -5.5 and (c) -1 °C

3. Results

3.1. Radiographic observations

In order to qualitatively capture the influence of thermal cycling, X-ray radiographic observations were performed by mounting the cold-stage inside the Phoenix v|tomelx X-ray equipment. Continuous radiographs were acquired during a thermal cycle but with a slower cooling rate of 0.1 K/min. Figure 4 shows the radiographic images of a 3 mm ice cream sample at three temperatures when heated to 0°C from -20°C at 0.1°C/min. During heating, the overall structure remained unchanged until about -6°C. Upon further heating gradual expansion and an increase in air cell volume was noticed. From the literature [2] the melting point of ice cream is around -3°C, and heating beyond -3°C resulted in partial melting and formation of a separation/void within the ice cream sample (Fig 4c). Further cycling has shown that the formation of a void is permanent, and thus showing that -3°C is a critical temperature to be avoided for thermal abuse. Note that in the radiographs, dark grey indicates a denser phase such as sugar/protein matrix and ice-crystals whereas the white indicates air-cells. The lighter shade of grey corresponds to fat/liquid phase. These observations were performed only for a qualitative understanding, whereas the tomographic reconstruction is known to enhance the contrast and enable better segmentation of the image, allowing identification of the distinct phases.

3.2. Tomographic observations and quantification

Based on the observations from the radiography study, thermal cycles were performed and tomographic scans were acquired at -20 °C as outlined in section 2.3. The images were reconstructed [15] and further processed with Avizo® (FEI-VSG, France). Figure 5 shows the sequence of images and a magnified region. The dark grey (black) colour corresponds to a phase with lowest density. Hence in these images the black colour represents air-cells, which are separately shown in the magnified views 5(d-f). The reconstructed volumes are then used to separate the air-cells from the rest of the matrix. The reconstructed images are filtered using Anisotropic diffusion filter, and thresholded to distinguish air cells from the rest of the sample. The connected air cells are separated using watershed separation algorithm [16]. Figures 5(g-i) show 3D rendering of separated air cells. It is evident that the thermal cycling has introduced significant coalescence and growth of air cells.

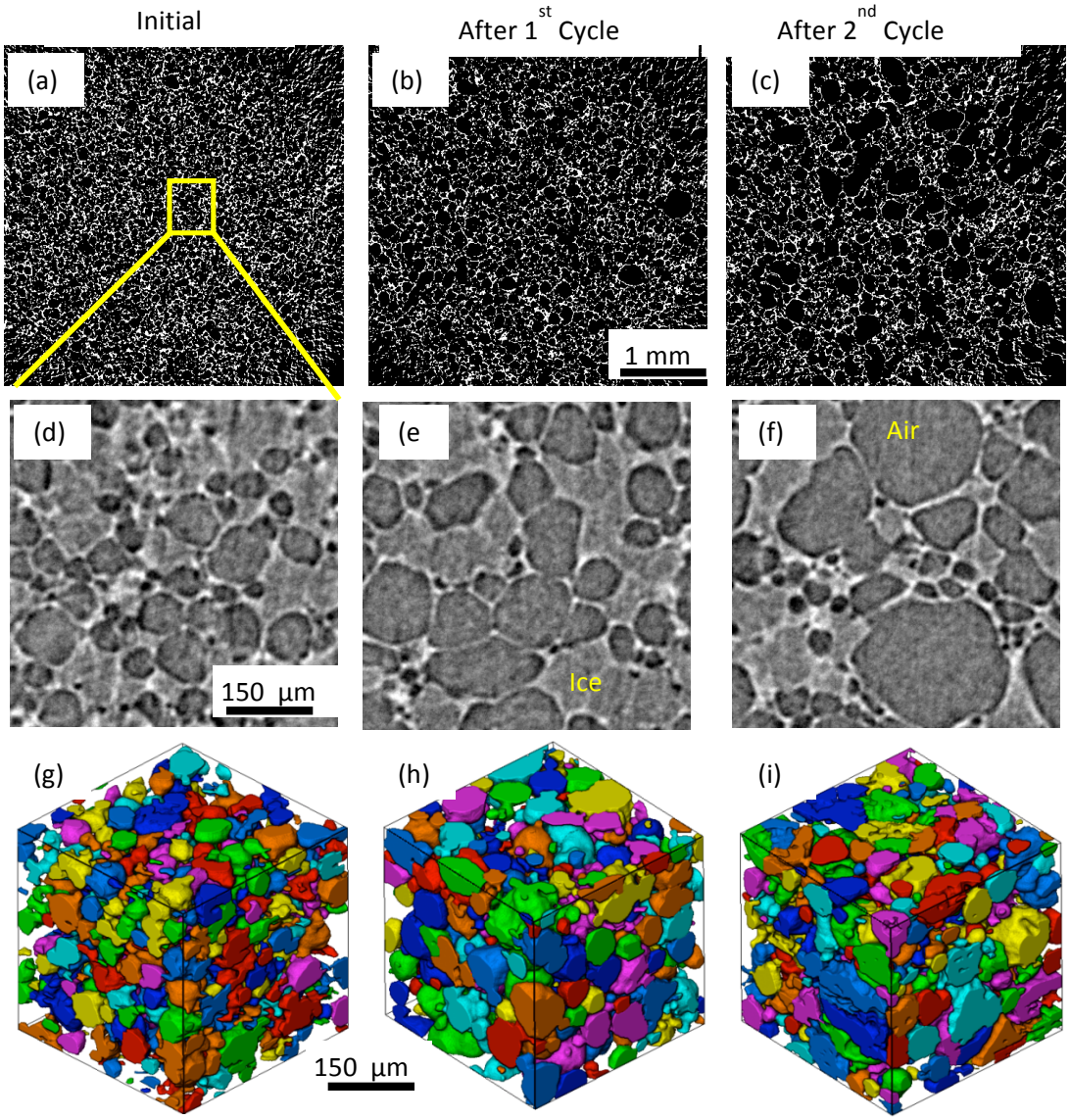

Fig 5: Image reconstruction and segmentation: (a-c) Reconstructed horizontal images from the tomography scan with 4× objective lens (d-f) A magnified view of a 640 × 640 μm^2 window, air-dark grey & ice crystals-light grey (g-i) Separated air-cells rendered in 3D during each stage

The volume fraction of air cells and their size distribution can be measured upon further quantification on a 1 mm^3 volume. The size distribution is shown in Fig. 6, with the mode in pore size increasing

after the first cycle from 75 to 135 μm equivalent pore diameter, with the number density in air bubbles continuous decreasing from initially 1976 to 1396 and 1263/ mm^3 after the first and second cycles respectively. This quantifies the effect of thermal cycling on the ice cream sample.

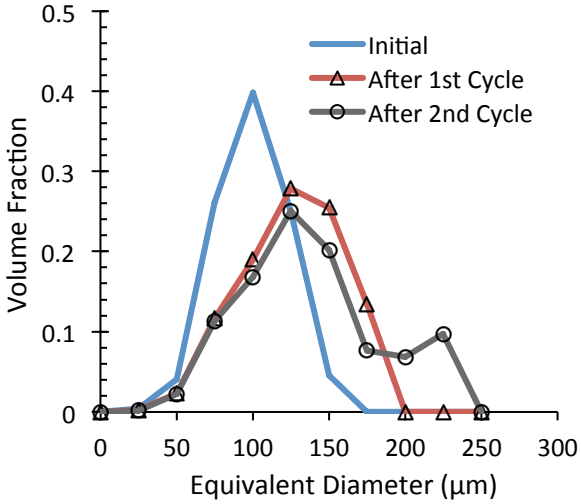

Fig 6: Size distribution of air cells in a 1 mm^3 volume as a function of cycling. The volume fraction of air cells during each stage is indicated in the legend.

Further analysis is required to investigate the effect of thermal cycling on the ice-crystals performed over a large number of cycles to represent industrial production and usage. We believe that the technique and capabilities presented in this work will enable these investigations not only on the ice cream but on a range of thermally controlled multi-phase soft materials.

4. Conclusions

This paper highlights a capability of capturing 4D observations on a multi-phase soft solids such as ice cream using synchrotron X-ray microtomography. The purpose built cold-stage is able to accurately control temperatures in the range of -40 to 20 °C. and allow simultaneous rotation of the specimen for tomographic imaging whilst maintaining a sealed environment. The results have shown successful tomographic imaging of ice cream samples subjected to thermal cycling from a base temperature of -20°C. Two thermal cycles are performed on the sample from -20 up to -7 °C at a constant rate of 0.3 °C/min. This has resulted in an increase in the equivalent diameter of air cells from 75 μm to 135 μm, with the number density decreasing from 1976 to 1263 /mm^3. The technique established here can be further utilized to not only understand the behaviour individual crystals with high resolution imaging but also to extend the methodology to analogous systems that are critical for food and polymer processing.

Acknowledgements

This work was made possible by the facilities and support provided by Unilever R&D, Colworth U.K, the Diamond Manchester Collaboration (beamtime MT11078-1) and the Research Complex at Harwell (EPSRC-EP/I02249X/1).

References

[1] Goff H D and Hartel R W 2013 *Ice Cream* (Springer)
[2] Clarke C 2012 *Science of Ice Cream* (Royal Society of Chemistry)
[3] Cook K L K and Hartel R W 2010 Mechanisms of Ice Crystallization in Ice Cream Production *Compr. Rev. Food Sci. Food Saf.* **9** 213–22
[4] Rau C, Weitkamp T, Snigirev A A, Schroer C G, Benner B, Tuemmler J, Guenzler T F, Kuhlmann M, Lengeler B, Krill III C E, Doebrich K, Michels D and Michels A 2002 Tomography with high resolution vol 4503 pp 14–22
[5] Lee P D and Hunt J D 1997 Hydrogen porosity in directional solidified aluminium-copper alloys: In situ observation *Acta Mater.* **45** 4155–69
[6] Kareh K M, Lee P D, Atwood R C, Connolley T and Gourlay C M 2014 Revealing the micromechanisms behind semi-solid metal deformation with time-resolved X-ray tomography *Nat Commun* **5** 4464
[7] Guillemot G, Gandin C-A and Bellet M 2007 Interaction between single grain solidification and macrosegregation: Application of a cellular automaton—Finite element model *J. Cryst. Growth* **303** 58–68
[8] Asta M, Beckermann C, Karma A, Kurz W, Napolitano R, Plapp M, Purdy G, Rappaz M and Trivedi R 2009 Solidification microstructures and solid-state parallels: Recent developments, future directions *Acta Mater.* **57** 941–71
[9] Yasuda H, Yamamoto Y, Nakatsuka N, Nagira T, Yoshiya M, Sugiyama A, Ohnaka I, Umetani K and Uesugi K 2008 In situ observation of nucleation, fragmentation and microstructure evolution in Sn-Bi and Al-Cu alloys *Int. J. Cast Met. Res.* **21** 125–8
[10] Bhreasail Á N, Lee P D, O'Sullivan C, Fenton C H, Hamilton R, Rockett P and Connolley T 2012 In-Situ Observation of Cracks in Frozen Soil using Synchrotron Tomography *Permafr. Periglac. Process.* **23** 170–6
[11] Appolaire B, Albert V, Combeau H and Lesoult G 1998 Free growth of equiaxed crystals settling in undercooled NH4Cl-H2O melts *Acta Mater.* **46** 5851–62
[12] Farup I, Drezet J and Rappaz M 2001 In situ observation of hot tearing formation in succinonitrile-acetone *Acta Mater.* **49** 1261–9
[13] Pinzer B R, Medebach a., Limbach H J, Dubois C, Stampanoni M and Schneebeli M 2012 3D-characterization of three-phase systems using X-ray tomography: tracking the microstructural evolution in ice cream *Soft Matter* **8** 4584
[14] Van Dalen G 2012 A Study of Bubbles in Foods by X-Ray Microtomography and Image Analysis *Microsc. Anal.* 26(2):S8–12 (AM)
[15] Titarenko S, Titarenko V, Kyrieleis A and Withers P J 2009 A ring artifact suppression algorithm based on a priori information *Appl. Phys. Lett.* **95** 071113
[16] Kareh K M, Lee P D and Gourlay C M 2012 In situ , time-resolved tomography for validating models of deformation in semi-solid alloys *IOP Conf. Ser. Mater. Sci. Eng.* **33** 012037